Core–Shell Nanostructures

Facile Fabrication of Inorganic-Polymer Core–Shell Nanostructures by a One-Step Vapor Deposition Polymerization**

Jyongsik Jang and Byungkwon Lim*

The enhanced stability and tunable surface properties derived from the selective polymer coating of inorganic colloids have expedited the development of a variety of methods to fabricate inorganic-polymer core–shell nanostructures.[1] To date, the preparation of polymer-coated inorganic nanoparticles has largely depended upon the solution-based approaches, which include emulsion or dispersion polymerization[2] and adsorption of polymers onto the inorganic particles.[3] However, these methods have often been limited by the large particle–particle aggregations, the formation of the isolated polymer particles from the inorganic colloids, or the requirement for the complicated multistep procedure. Therefore, it is desirable to develop a simple and reliable method to fabricate inorganic colloid-polymer nanoparticles with the well-defined core–shell morphology. Vapor deposition techniques can provide the creation of a smoother and more uniform polymer layer by the consecutive polymerization of vaporized monomer under a vacuum onto the desired surface. While vapor deposition polymerization (VDP) has been performed on the metal and semiconductor with macroscopically flat surfaces by radiation-induced polymerization,[4] considerably less attention has been paid to the coating of inorganic colloids with polymers. Herein we report a facile route for the fabrication of various inorganic colloid-vinyl polymer core-shell nanostructures by one-step VDP. Having demonstrated the feasibility of the above approach, we were prompted to apply it to encapsulate silica and titania nanoparticles with poly(methyl methacrylate) (PMMA) and polydivinylbenzene (PDVB).

Spherical silica colloids of two different sizes (200 and 25 nm) and irregularly shaped titania nanoparticles were used as the cores and pretreated with a silane coupling agent to improve the chemical affinity of the inorganic particle surfaces towards organic monomers. The surface-modified inorganic colloids were encapsulated with two vinyl polymers; PMMA as an optically transparent material, and PDVB as a carbon precursor. The overall synthetic procedure is represented in Scheme 1. The reactor containing the inorganic nanoparticles and a solid initiator was evacuated at room temperature until the pressure inside reached about 10^{-1} Torr,

[*] Prof. Dr. J. Jang, B. Lim
Hyperstructured Organic Materials Research Center and
School of Chemical Engineering
Seoul National University
Shinlimdong 56-1, Seoul 151-742 (Korea)
Fax: (+82) 2-888-1604
E-mail: jsjang@plaza.snu.ac.kr

[**] This work was supported by the Brain-Korea 21 Program of the Korea Ministry of Education and by Hyperstructured Organic Materials Research Center in Seoul National University.

  DOI: 10.1002/ange.200352113

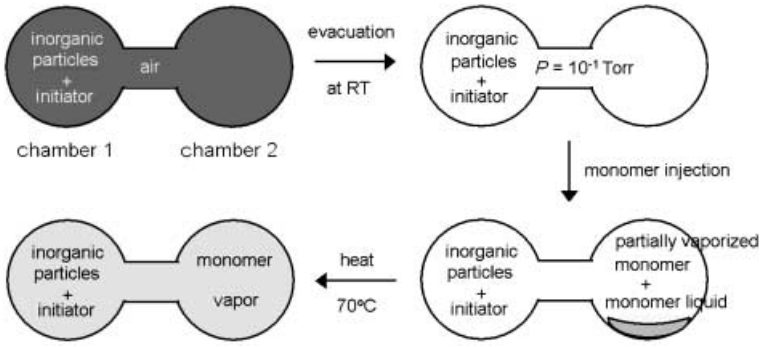

Scheme 1. Illustration of the VDP for the encapsulation of the inorganic nanoparticles.

which put the system under a static vacuum. Then, liquid monomer was introduced into the reactor by injection. The monomers were partially vaporized as soon as they were injected inside the reactor at room temperature and completely vaporized by heating the reactor at 70 °C. Polymerization was initiated by thermal decomposition of a radical initiator and the inorganic particles were stirred with a magnetic to prevent the formation of particle–particle aggregations.

In the case of 200 nm sized silica colloid-PMMA nanocomposites, FTIR spectrum indicated PMMA C–H stretching bands at 2957 cm^{-1} and 3000 cm^{-1} and a carbonyl stretching band at 1737 cm^{-1} as well as the characteristic peaks of silica at 3400, 1630, 1100, 956, and 474 cm^{-1}. The C=C stretching band at 1620 cm^{-1} from the MMA monomer disappeared after polymerization. An X-ray photoelectron spectroscopy (XPS) study showed the C 1s peak at 284 eV and O 1s peak at 533 eV with a shoulder at 531 eV. The XPS spectrum of the pure silica particles showed the O 1s peak of the symmetrical shape near at 533 eV with no shoulder peak. Therefore, XPS confirmed the presence of carbon and oxygen atoms originating from PMMA. Thermogravimetric analysis (TGA) showed that PMMA decomposed completely below 500 °C. These results demonstrate the successful polymerization of methyl methacrylate (MMA) and also the availability of a radical initiator for the initiation of the VDP.[5]

A scanning electron microscopy (SEM) image shows 200 nm spherical silica particles (Figure 1 a). PMMA-coated silica nanoparticles obtained with an MMA/silica weight ratio of 0.25 are shown in Figure 1 b. These nanoparticles have a morphology similar to silica particles, thus indicating uniform PMMA layers on the silica particle surfaces. In transmission electron microscopy (TEM) images, the PMMA-coated silica particles have a uniform and remarkably thin PMMA layer (shell thickness 8 nm) on their outer surface (Figure 1 c and 1 d). In addition, we did not observe the polymer particle that had not encapsulated the inorganic particle in TEM investigation. The formation of the highly uniform PMMA layer and the absence of polymer particles might result from the nature of the VDP and the high specific surface area of inorganic nanoparticles to be encapsulated. The inorganic nanoparticles provide the considerably large surfaces even with a small number of particles compared to semiconductor or metallic flat surfaces, on which the most of monomers can adsorb from the vapor phase. Under these conditions, polymerization of the monomers proceeds exclusively by growing polymer radicals confined in the adsorbed layers and is not significantly affected by polymerization in the gas phase.[6] The growth of the polymer layer in the particle surfaces leads to the formation of the highly uniform polymer shell.

The degree of polymerization depended on the reaction time, the initiators, and the reaction temperature. In the control of the thickness of the polymer, we selected the loading amount of the monomer as a control parameter and fixed other reaction parameters to simplify the reaction system such as the reaction time of 24 h and the reaction temperature of 70 °C. The shell thickness could be tuned by varying the MMA/silica weight ratio. As the MMA/silica weight ratio increased, the polymer shell thickness increased gradually. The PMMA shell thickness of about 25 nm was obtained with an MMA/silica weight ratio of 0.75 (Figure 1 e) and increased up to about 39 nm at the weight ratio of 1.5 (Figure 1 f). VDP provided a uniform PMMA shell regardless of the increment in shell thickness.

The VDP method was also applied to encapsulate colloidal silica less than 50 nm. It was found that the aggregation of particles during the polymerization often occurred with higher quantities of monomer, without stirring the inorganic particles, especially in the coating of nano-

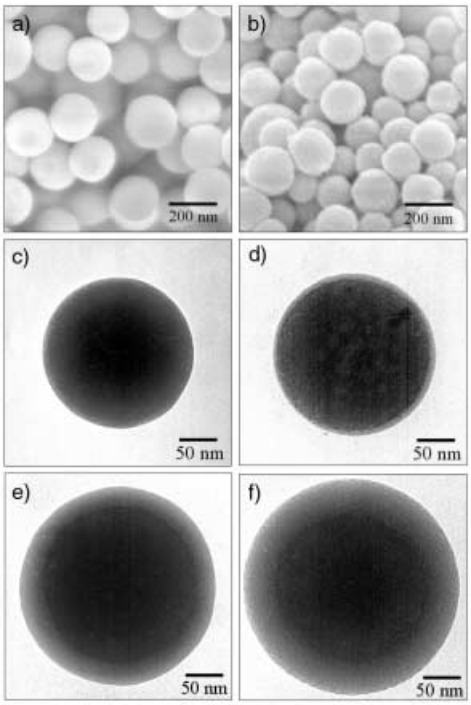

Figure 1. SEM images of a) 200 nm silica particles as synthesized and b) silica particles coated with PMMA. TEM images of c) 200 nm silica particle and d–f) silica–PMMA core–shell nanoparticles with the various shell thickness (MMA/silica weight ratio of 0.25 in d), 0.75 in e), and 1.5 in f).

particles less than 50 nm compared to that of relatively large nanoparticles of 200 nm in diameter. However, the particle–particle aggregations were remarkably reduced by stirring the nanoparticles during polymerization and by using the appropriate choice of synthetic conditions. Stirring of the particles decreases the contact time between the neighboring particles so that it effectively prevents the formation of the polymer layer connecting the inorganic particles. Figure 2a and b

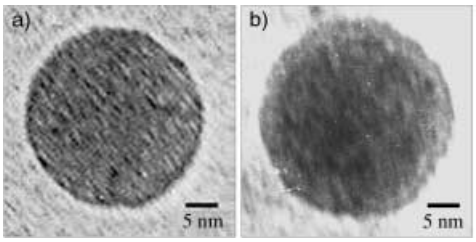

Figure 2. TEM images of a) 25 nm silica particle and b) PMMA-coated silica particle with the shell thickness of about 2.5 nm.

represent the highly magnified TEM images of 25 nm silica colloids before and after the deposition of PMMA with an MMA/silica weight ratio of 0.75 at 70 °C. Figure 2b shows the outer shell of the particle brighter than the dark inner core, which confirms the silica–PMMA core–shell nanostructure. The shell thickness of PMMA was about 2.5 nm. Our results show that the core–shell morphology can be obtained with the silica particles as small as 25 nm.

Titania is well-known for its use in optical and photocatalytic applications. In our experiment, titania nanoparticles of irregular shapes were encapsulated with a PMMA shell to improve their stability and dispersibility for a variety of applications. The representative TEM micrograph of titania–PMMA nanoparticles (MMA/titania weight ratio of 1.5; Figure 3) proved that 200 nm titania nanoparticles were

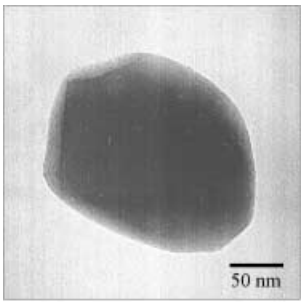

Figure 3. TEM image of titania–PMMA core–shell nanoparticle. The titania nanoparticle was completely encapsulated with the PMMA layer.

successfully coated with a PMMA shell, and the shell had the same morphology as that of the titania nanoparticles. The shell thickness ranged from 10 to 20 nm. This result suggests that VDP is also available for the encapsulation of the irregularly shaped inorganic particles as well as spherical silica particles.

PDVB is a typical crosslinked polymer and can be used as a carbon precursor. Figure 4a presents the TEM image of the silica–carbon core-shell nanoparticle with a shell thickness of about 15 nm, which was prepared by the carbonization of the

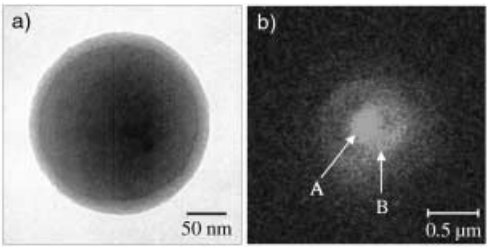

Figure 4. a) TEM image of silica-carbon core-shell nanoparticle and b) CLSM fluorescence image of pyrene-encapsulated hollow carbon nanoparticle. Green emission results from pyrene. The emission in region A originates from pyrene inside the carbon capsule and that in region B from pyrene adsorbed on the outer surface of carbon capsule.

silica–PDVB core-shell nanoparticle. Carbon nanocapsules were obtained by HF etching of the silica core. TGA of the carbon capsules confirmed that the residual amount of sample was less than 5 wt % under an oxygen flow and confirmed the successful removal of the silica. This fact also implies that the wall of carbon capsule is porous and permeable towards small molecules.[7] The carbon capsule was used as a host container for the encapsulation of pyrene, a photochromic dye material. The confocal-laser scanning microscope (CLSM) image of pyrene-embedded carbon capsule dispersed in water showed a green emission resulting from the pyrene molecules (Figure 4b). It is noticeable that the pyrene emission could be divided into two, that is, one originating from pyrene molecules inside the carbon capsule (labeled A in Figure 4b), and the other with a donut shape originating from pyrene molecules adsorbed on the outer surface of the carbon capsule (labeled B in Figure 4b). The diameter of the emission from the region A was about 200 nm, which was in good agreement with the size of the capsule core. When the CLSM observation was performed in benzene instead of water, the pyrene emission was no longer concentrated in the carbon capsule, but displayed from the entire benzene media. This is because hydrophobic pyrene tends to locate at the hydrophobic interior of the carbon capsule in water, but the encapsulated pyrene is released from the carbon capsule in hydrophobic benzene. This result indicates the potential of the carbon capsule as the container for storage and release of organic guest molecules in a different environment.

In summary we have demonstrated the VDP methodology as a new strategy to fabricate various inorganic colloid–vinyl polymer core–shell nanostructures. This conceptually new and simple process has allowed the formation of highly uniform PMMA shells on silica and titania nanoparticle surfaces. The shell thickness could be controlled from about 2.5 to 40 nm by changing the monomer/inorganic particle weight ratio. In addition, carbon capsules derived from the silica–PDVB nanoparticles realized the encapsulation and selective release property of pyrene in a different environment and can be applied as a novel nanohybrid material in

optical and electronic devices. This novel approach might be expanded to allow the preparation of the various core–shell structures, which include metallic, inorganic, and polymeric materials.

Experimental Section

Uniform silica spheres of about 200 nm were synthesized according to the method of Stöber et al.[8] Ludox TM-40 solution (Aldrich) was used as a source of 25 nm silica nanoparticle. Titanium dioxide (Junsei Chemical) was chosen as 200 nm titania nanoparticles. Silica and titania nanoparticles (2 g) were treated with chlorodimethylvinylsilane (CDVS, 0.2 mL) in a mixture solution of ethanol (75 mL) and water (15 mL) overnight, and then dried at 50 °C. A reactor was designed for VDP by connecting two modified round bottom flasks as reaction chambers. The total volume of the reactor was about 200 mL. 0.3 g of CDVS-treated inorganic particle and 0.01 g of a radical initiator was added to the one chamber of the reactor. 2,2′-azobis-[2-(2-imidazolin-2-yl)-propane] dihydrochloride or 2,2′-azobisisobutyronitrile (AIBN) was used as a radical initiator. The reactor was evacuated to about 10^{-1} torr at room temperature, and then the vacuum valve was closed to obtain the system in a static vacuum. Liquid monomer was introduced into the other chamber of the reactor by injection (0.075–0.6 mL). The monomer was completely vaporized by heating at 70 °C. The vapor deposition polymerization proceeded with magnetic stirring of the inorganic particles in an atmosphere of the monomer vapor for 24 h. After the polymerization, the residual monomer vapor was removed from the reactor by venting and the final product of inorganic-polymer core-shell nanoparticle was obtained.

The silica–PDVB core–shell nanoparticles were carbonized under N_2 gas flow. The sample was heated up to 900 °C at a heating rate of 3 °C min^{-1}, held at that temperature for 5 h, and then cooled to room temperature. Carbon capsule was prepared by removal of the silica core with HF solution. To obtain pyrene-embedded carbon nanocapsule, pyrene (1 mg) in THF (1 mL) was introduced into the mixture of carbon nanocapsule (2 mg) in water (10 mL), and then vigorously stirred for 30 min. TEM and SEM images were taken by a JEOL 2010 high-resolution microscope and a JEOL 6700F field emission scanning electron microscope, respectively. Fluorescence image of pyrene–carbon nanoparticle was obtained by using a Carl Zeiss LSM510 confocal laser scanning microscope. XPS spectra were recorded using Kratos Model AXIS-HS system. An $Al_{K\alpha}$ X-ray source was operated at a power of 100 W (10 mA and 10 kV). Infrared spectra were recorded on a Bomem MB 100 Fourier Transform Infrared (FTIR) Spectrometer with a transmission technique.

Received: June 11, 2003
Revised: September 3, 2003 [Z52113]

Keywords: colloids · nanostructures · polymers · silicon · titanium

[1] F. Caruso, *Adv. Mater.* **2001**, *13*, 11 – 22.
[2] a) L. Quaroni, G. Chumanov, *J. Am. Chem. Soc.* **1999**, *121*, 10642 – 10643; b) C. Barthet, A. J. Hickey, D. B. Cairns, S. P. Armes, *Adv. Mater.* **1999**, *11*, 408 – 410; c) S. Reculusa, C. Poncet-Legrand, S. Ravaine, S. Mingotaud, E. Duguet, E. Bourgeat-Lami, *Chem. Mater.* **2002**, *14*, 2354 – 2359; d) J. Luna-Xavier, A. Guyot, E. Bourgeat-Lami, *J. Colloid Interface Sci.* **2002**, *250*, 82 – 92.
[3] a) F. Caruso, R. A. Caruso, H. Möhwald, *Science* **1998**, *282*, 1111 – 1114; b) E. Donath, G. B. Sukhorukov, F. Caruso, S. A. Davis, H. Möhwald, *Angew. Chem.* **1998**, *110*, 2324 – 2327; *Angew. Chem. Int. Ed.* **1998**, *37*, 2202 – 2205.
[4] a) M. A. Bruk, S. A. Pavlov, A. D. Abkin, *Radiat. Phys. Chem.* **1981**, 17, 113 – 117; b) M. A. Bruk, K. K. Chuiko, A. D. Abkin, S. V. Kirpikov, *Polym. Sci. U.S.S.R.* **1982**, 24, 696 – 703; c) M. A. Bruk, S. V. Kirpikov, *Polym. Sci. U.S.S.R.* **1988**, 30, 130 – 136; d) J. Bai, C. M. Snively, W. N. Deglass, J. Lauterbach, *Macromolecules* **2001**, *34*, 1214 – 1220; e) J. Bai, C. M. Snively, W. N. Deglass, J. Lauterbach, *Adv. Mater.* **2002**, *14*, 1546 – 1549.
[5] a) J. Jang, B. Lim, J. Lee, T. Hyeon, *Chem. Commun.* **2001**, 1, 83 – 84; b) K. Moller, T. Bein, R. X. Fischer, *Chem. Mater.* **1998**, *10*, 1841 – 1852.
[6] M. A. Bruk, S. V. Kiroikov, *Colloid J.* **1995**, 57, 160 – 165.
[7] J. Jang, B. Lim, *Adv. Mater.* **2002**, *14*, 1390 – 1393.
[8] W. Stöber, A. Fink, E. Bohn, *J. Colloid Interface Sci.* **1968**, *26*, 62 – 69.

